# Auger optimization in mid-infrared lasers: the importance of final-state optimization

**Michael E. Flatté**

*Department of Physics and Astronomy, University of Iowa, Iowa City, IA 52242*

*michael-flatte@uiowa.edu*

**C. H. Grein**

*Physics Department M/C 273, University of Illinois at Chicago, Chicago, Illinois 60607-7059*

*grein@uic.edu*

**Abstract:** We consider the effect of reducing the density of final hole states for Auger processes on the Auger rate at room temperature and 77K at densities near lasing thresholds. The system of interest is a strain-compensated superlattice based on the InAs/GaInSb material system with a 3.7 $\mu$m band gap. At 77K the Auger lifetime is reduced by two orders of magnitude, while the change at 300K is less than a factor of two. We conclude that final-state optimization in this particular structure, while pronounced at 77K, has little effect at 300K.



**OCIS codes:** (140.5960) Semiconductor lasers; (140.3070) Infrared and far-infrared lasers; (999.9999) Auger recombination

## References

1. E. Yablonovitch and E. O. Kane, "Reduction of Lasing Threshold Current Density by the Lowering of Valence Band Effective Mass", *J. Lightwave Technol.* **LT-4**, 504 (1986).
2. *e.g.* L. A. Coldren and S. W. Corzine, *Diode Lasers and Photonic Integrated Circuits* (Wiley, New York, 1995).
3. T. C. Hasenberg, R. H. Miles, A. R. Kost, and L. West, "Recent advances in Sb-based midwave-infrared lasers", *J. Quantum Electron.* **QE-33**, 1403 (1997).
4. D. H. Chow, R. H. Miles, T. C. Hasenberg, A. R. Kost, Y.-H. Zhang, H. L. Dunlap, and L. West, "Mid-wave infrared diode lasers based on GaInSb/InAs and InAs/AlSb superlattices", *Appl. Phys. Lett.* **67**, 3700 (1995).
5. J. R. Meyer, C. A. Hoffman, F. J. Bartoli, and L. R. Ram-Mohan, "Type II quantum-well lasers for the mid-wavelength infrared", *Appl. Phys. Lett.* **67**, 757 (1995).
6. H. K. Choi, G. W. Turner, and M. J. Manfra, "High CW power (>200mW/facet) at 3.4$\mu$m from InAsSb/InAlAsSb strained quantum well diode lasers", *Electron. Lett.* **32**, 1296 (1996).
7. H. K. Choi, G. W. Turner, M. J. Manfra, and M. K. Connors, "175K continuous wave operation of InAsSb/InAlAsSb quantum-well diode lasers emitting at 3.5$\mu$m", *Appl. Phys. Lett.* **68**, 2936 (1996).
8. S. R. Kurtz, R. M. Biefeld, A. A. Allerman, A. J. Howard, M. H. Crawford, and M. W. Pelczynski, "Pseudomorphic InAsSb multiple quantum well injection laser emitting at 3.5 $\mu$m", *Appl. Phys. Lett.* **68**, 1332 (1996).
9. M. E. Flatté, J. T. Olesberg, S. A. Anson, T. F. Boggess, T. C. Hasenberg, R. H. Miles, and C. H. Grein, "Theoretical Performance of Mid-Infrared Broken-Gap Multilayer Superlattice Lasers", *Appl. Phys. Lett.* **70**, 3212 (1997). The layer widths of the four-layer superlattice given in this reference are in error — in fact they should be the same as those of the superlattice considered here.
10. M. E. Flatté, C. H. Grein, and H. Ehrenreich, "Sensitivity of optimization of mid-infrared InAs/InGaSb laser active regions to temperature and composition variations", *Appl. Phys. Lett.* in press.

#2830 - $15.00 US Received October 8, 1997; Revised February 12, 1998

11. C. H. Grein, P. M. Young, M. E. Flatté, and H. Ehrenreich, "Long wavelength InAs/InGaSb infrared detectors: Optimization of carrier lifetimes", *J. Appl. Phys.* **78**, 7143 (1995).

12. M. E. Flatté, C. H. Grein, H. Ehrenreich, R. H. Miles, and H. Cruz, "Theoretical performance limits of $2.1 - 4.1$ $\mu$m InAs/InGaSb, HgCdTe, and InGaAsSb lasers", *J. Appl. Phys.* **78**, 4552 (1995).

13. M. E. Flatté, P. M. Young, L.-H. Peng, and H. Ehrenreich, "Generalized superlattice $\mathbf{K}\cdot\mathbf{p}$ theory and intersubband optical transitions", *Phys. Rev. B* **53**, 1963 (1996).

14. O. Madelung, in *Semiconductors, Physics of Group IV Elements and III-V Compounds*, edited by K.-H. Helluege and O. Madelung, Landolt-Börnstein, New Series, Group III, Vol. 17, Pt. a (Springer-Verlag, Berlin, 1982).

15. O. Madelung in *Intrinsic Properties of Group IV Elements and III-V, II-VI and I-VII Compounds*, edited by K.-H. Helluege and O. Madelung, Landolt-Börnstein, New Series, Group III, Vol. 22, Pt. a (Springer-Verlag, Berlin, 1987).

16. M. E. Flatté, C. H. Grein, T. C. Hasenberg, S. A. Anson, D.-J. Jang, J. T. Olesberg, and T. F. Boggess, "Carrier recombination rates in narrow-gap semiconductor superlattices", unpublished.

---

Carrier recombination in room-temperature high-quality semiconductors with band gaps in the mid-infrared and carrier densities sufficient for lasing is typically dominated by direct Auger processes. In such a process a pair recombines and transfers its energy and momentum to another electron (electron Auger process) or another hole (hole Auger process). Strategies to reduce Auger rates through "band-structure engineering" can be placed into several categories: (1) band-edge optimization, characterized by attempts to reduce the band-edge density of states of the valence band, (2) intersubband absorption reduction, and (3) final-state optimization, characterized by attempts to eliminate final states for the carrier excited during the pair recombination process.

Band-edge optimization works because the threshold carrier density decreases when the valence band density of states decreases[1]. Since the Auger rate per pair depends strongly on the carrier density (as $n^2$ for equal densities of electrons and holes in the non-degenerate regime), the reduced threshold carrier density directly translates into a reduced threshold current density. Even if the recombination rate per pair is not dominated by Auger processes, it typically increases at higher carrier densities, and so reducing the threshold carrier density has motivated the use of strained heterostructure lasers in several wavelength ranges[2]. Strain lifts the heavy-light hole degeneracy at the valence band edge and thus makes the heavy-hole's in-plane mass light, implying a lower band-edge density of states. This lower band-edge density of states induces a lower threshold carrier density, a longer carrier lifetime, and, as a final result, a lower threshold current density. In the mid-infrared several types of material systems incorporating strain have been explored[3−8].

Strategies for intersubband absorption reduction focus on eliminating intervalence or interconduction transitions at energies equal to the lasing energies. By reducing these loss mechanisms the threshold carrier density is reduced. Just as described above in the case of band-edge optimization, a reduced threshold carrier density implies a longer carrier lifetime and a lower threshold current density. This strategy is realized by designing a structure with gaps in the valence band states for small in-plane momentum and at energies near a lasing energy above the conduction minimum and a lasing energy below the valence maximum. This procedure has been successfully applied to systems in the mid-infrared[9,10].

Final-state optimization relies on the non-equilibrium electrons and holes being most concentrated at zero in-plane momentum while the available final states have substantial in-plane momentum. In this situation, nonequilibrium electrons and holes from regions of low occupation (substantial in-plane momentum) are required for the Auger

#2830 - $15.00 US Received October 8, 1997; Revised February 12, 1998

process. Final-state optimization, first applied to long-wavelength infrared detectors[11], works best at low density, when the nonequilibrium electrons and holes are closest to the band edges. In long-wavelength infrared detectors the carrier lifetime of band-edge minority carriers was increased by several orders of magnitude. The purpose of this Letter will be to evaluate the importance of final-state optimization for mid-infrared strained semiconductor superlattices at 77K and 300K and at the carrier densities required for gain at those temperatures. Previous studies of active region optimization compared different material systems[12] or examined sensitivity of a design to the ambient temperature or to growth errors in layer thicknesses[10], but did not separate cleanly the effect of band-edge optimization from final-state optimization in a particular model system. We note, however, that our conclusions are limited to one particular wavelength and type of active region.

As a model system we consider a strain-compensated broken-gap superlattice[9] with a 300K emission wavelength of 3.7 $\mu$m, 13.8Å InAs/24Å $Ga_{0.60}In_{0.40}Sb$/13.8Å InAs/40Å $Al_{0.30}Ga_{0.42}In_{0.28}As_{0.50}Sb_{0.50}$. The band structure of this superlattice exhibits final-state optimization; namely, it has a gap in the growth-axis final states at certain crucial energies (so-called resonance energies). These resonance energies are located $E_g$ below the valence maximum and $E_g$ above the conduction minimum, where

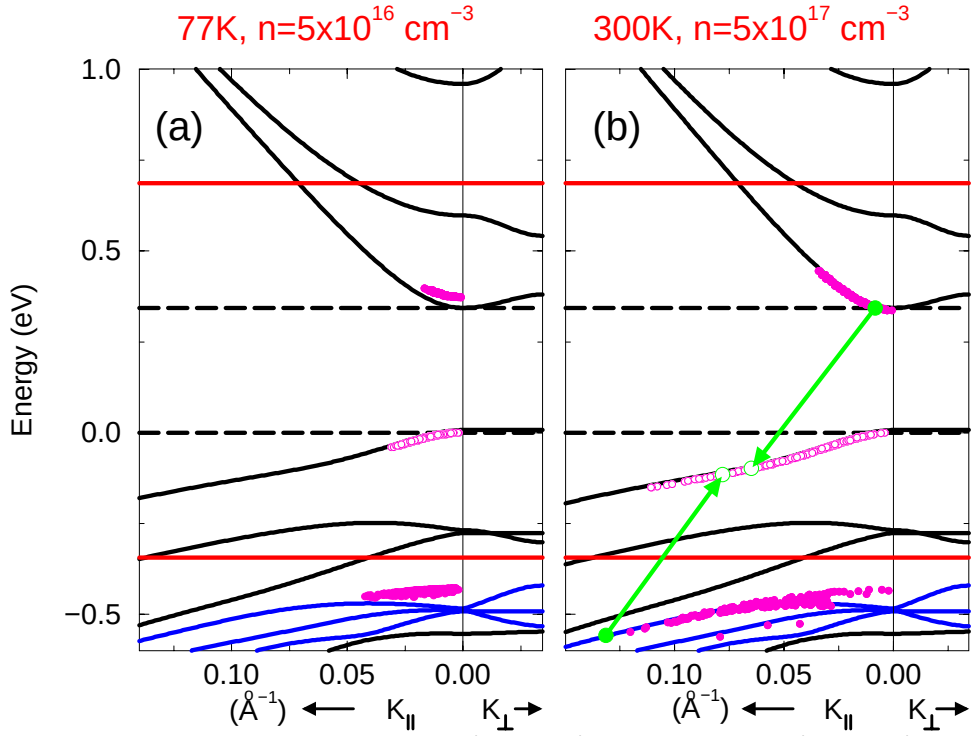


Figure 1. Band structure for a 13.8Å InAs/24Å $In_{0.40}Ga_{0.60}Sb$/13.8Å InAs/40Å $Al_{0.30}In_{0.28}Ga_{0.42}As_{0.50}Sb_{0.50}$ superlattice at a lattice temperature of 300K. The in-plane momentum is $K_{||}$ while the growth-direction momentum is $K_{\perp}$. Resonance energies within the conduction band and valence band are shown by solid red lines. The subbands which contribute most to the hole Auger rate are indicated in blue. Dashed lines mark the conduction and valence edge energies. The electrons (filled magenta circles) and holes (empty magenta circles) involved in the (roughly) 500 most probable transitions at (a) 77K and $n = 5 \times 10^{16}$ cm$^{-3}$ and (b) 300K and $n = 5 \times 10^{17}$ cm$^{-3}$ are also shown. In (b) the single most probable transition is shown in green schematically

#2830 - $15.00 US
Received October 8, 1997; Revised February 12, 1998

$E_g$ is the fundamental gap. (The intersubband absorption of this structure at the lasing energy is also minimal — note that the resonance energies are also (roughly) the relevant energies for intersubband absorption[9].) The band structure of this superlattice is shown in Fig 1, and the resonance energies are indicated by red lines. Final states in the valence band (for hole Auger) must lie below the red line at $E_V - E_g$, while final states in the conduction band (for electron Auger) must lie above the red line at $E_C + E_g$.

Calculations of the electronic structure of the superlattice considered here were performed with an envelope-function approximation and using a superlattice $\mathbf{K} \cdot \mathbf{p}$ technique similar to that used in Refs. 12 and 13 but generalized to an arbitrary number of layers in the unit cell. Parameters (with the exception of the energy gap) of the bulk materials comprising the superlattice layers are linearly interpolated from binary constituents. The valence band offsets are also largely linearly interpolated. The experimental parameters are obtained principally from Refs. 14 and 15, and are tabulated in Ref. 12. The single exception is the energy of the conduction band in the quinternary, which occurs (including strain effects) 1.045 eV above the InAs conduction band. The Auger rates are evaluated according to the formalism described in detail in Ref. 11, with the recent addition of Umklapp processes, which contribute about half of the total direct Auger rate[16].

In order to examine final-state optimization we focus entirely on hole Auger. Strong experimental evidence based on the density dependence of the rate indicates that the hole Auger rate dominates in this structure[16]. Calculations indicate the electron Auger rate to be more than 3 times smaller than the hole Auger rate at 300K lasing densities. This may not be the case in other mid-infrared laser active regions.

There is a substantial gap (140 meV in Fig. 1(a,b)) in the valence band around the resonance energy for momenta along the growth direction ($K_\perp$). States do reside at the resonance energy, however, for finite in-plane momentum ($K_\parallel$). The subbands most involved as final states for hole Auger are those directly under the resonance energy line, and are shown in blue. Also shown are the (roughly) 500 most probable hole Auger transitions as a function of *in-plane* momentum at typical lasing threshold carrier densities at 77K (Fig. 1(a)) and 300K (Fig. 1(b)). The electrons involved in this process are indicated by filled magenta circles, while the holes are indicated by empty magenta circles. The single most probable process is shown in Fig. 1(b) schematically in green. The process whereby the equilibrium electron deep within the valence band eliminates a band-edge hole can also be understood as a band-edge hole being excited to a higher-energy state. The momentum of this final-state hole is the sum of the momenta of the initial pair and the extra band-edge hole.

The elimination of band-edge Auger processes due to final-state optimization does occur at 77K and does reduce the Auger rate. The non-equilibrium electrons in the conduction band which are involved in Auger processes (shown in Fig. 1(a)) are clearly at higher energy than the band minimum. Their energy difference is roughly 30 meV, which corresponds to $\sim 4k_BT$. Since the occupation factors are proportional to $\exp(-E/k_BT)$, this energy difference produces a reduction in the occupation factor of two orders of magnitude. Since the hole Auger rate is directly proportional to that occupation factor, the hole Auger rate is also reduced by two orders of magnitude.

The situation at 300K is shown in Fig. 1(b). Due to the marked sensitivity of the Auger rate on band gap the differences in the band structure at 77K and 300K are ignored; as a control we use the 300K band structure for both carrier temperatures. Whereas the nonequilibrium carriers were quite concentrated at the zone center at 77K, at 300K they are substantially more spread out. In addition, the non-equilibrium electrons involved in the most probable transitions are located at the conduction band minimum. Hence the contribution of final-state optimization to reducing the Auger rate

#2830 - $15.00 US Received October 8, 1997; Revised February 12, 1998

at 300K seems likely to be small.

Our procedure is to take the band structure shown in Fig. 1(a,b) and manually shift the fourth, fifth and sixth valence subbands from the valence edge (shown in blue in Fig. 1(a,b)) in energy and observe the effect on the carrier lifetimes. As the bands are shifted up more states at zero in-plane momentum become accessible as final states for Auger processes. We show in Fig. 2 the 500 most probable transitions for the same situation as Fig. 1, but with the three subbands (shown in blue) shifted up by 90 meV at 77K (Fig. 2(a)) and 100 meV at 300K (Fig. 2(b)). Immediately evident in Fig. 2(a) is that the electrons (filled magenta circles) in the conduction band which were 30meV above the band edge in Fig. 1(a) are now at the band edge. Hence the final-state optimization has been removed. At 300K, in contrast, there is little difference.

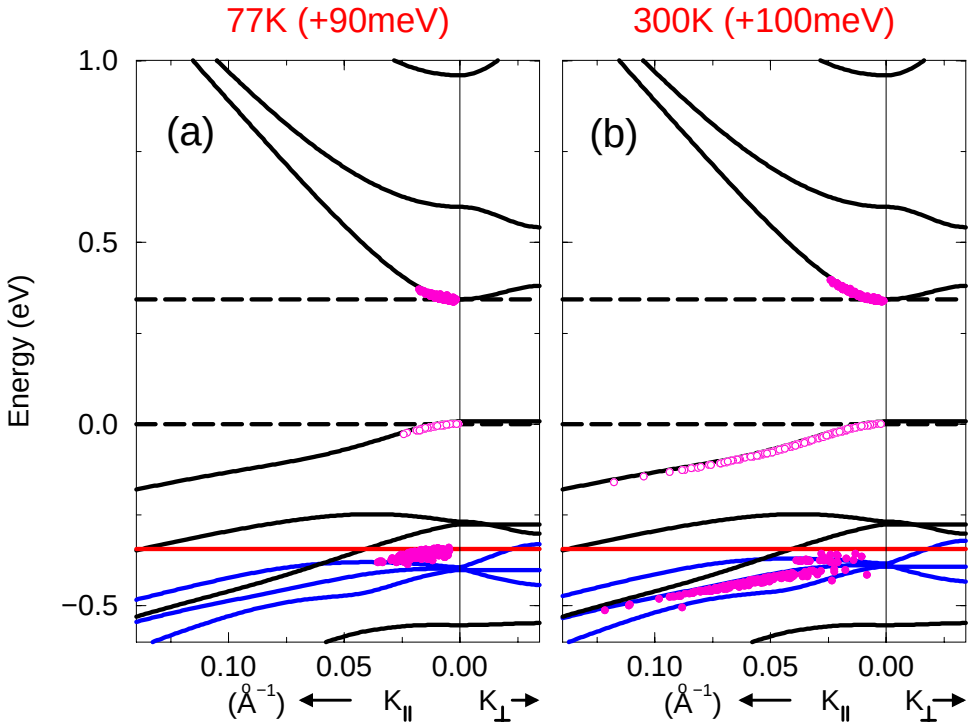


Figure 2. Same as Fig. 1, but with the most important (blue) subbands shifted up in energy by (a) 90 meV and (b) 100 meV. Only the valence resonance energy is shown (red).

Fig. 3 shows the carrier lifetime as a function of the energy shift of the bands towards the band edge. The lifetime becomes long for large positive energy shifts, for the relevant bands eventually become shifted above the resonance energy, and thus cannot contribute to the Auger rate. The lifetime also becomes long for large negative energy shifts because the subbands become too far below the resonance energy to be accessible for Auger processes involving band-edge nonequilibrium electrons and holes. It is particularly the latter situation we are interested in, for it is the essence of final-state optimization.

The behavior for small shifts is markedly more pronounced at 77K than at 300K. Whereas at 77K the difference in Auger rate between the 77K band structures of Fig. 1(a) and Fig. 2(a) is over two orders of magnitude, the difference in Auger rate between the 300K band structures of Fig. 1(b) and Fig. 2(b) is less than a factor of two. In fact, the design of Fig. 1(b), which was intended to have a long Auger lifetime, has a

#2830 - $15.00 US
Received October 8, 1997; Revised February 12, 1998

lifetime which is near the minimum calculated. The Auger suppression of Fig. 1(a) arises because the final states of the three blue subbands are sufficiently low in energy to be difficult for band-edge electrons and holes to use as final states. At 300K a structure with a resonance energy gap 100 meV larger than Fig. 1(b) (corresponding to a −100 meV shift of the bands in Fig. 3(b)) would have a hole Auger rate suppressed by one order of magnitude simply from final-state effects.

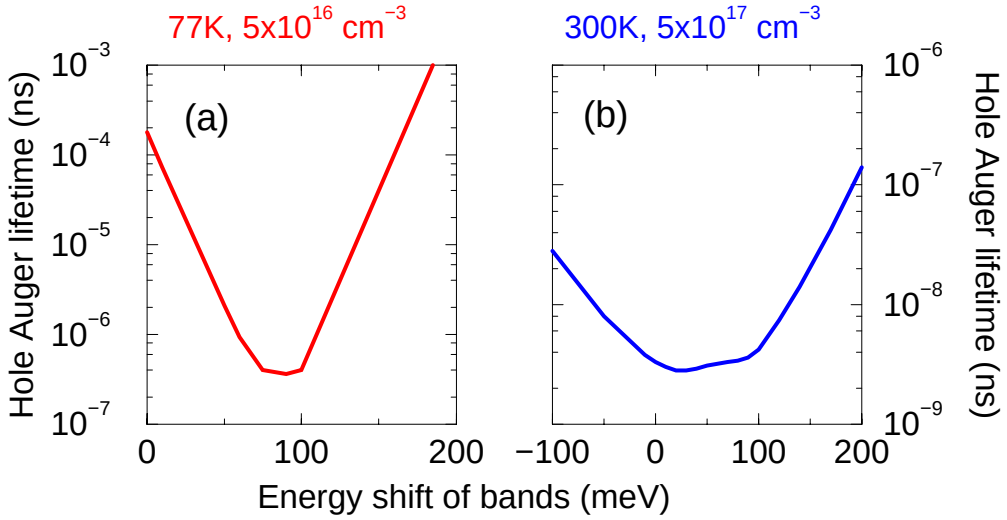


Figure 3. Hole Auger lifetime as a function of the energy shift of the fourth, fifth and sixth valence subbands towards the band edge (a) at 77K and a density of $5 \times 10^{16}$ cm$^{-3}$ and (b) at 300K and a density of $5 \times 10^{17}$ cm$^{-3}$.

We can estimate the width of the lifetime minimum in Fig. 3(a,b) from the spread of the electron and hole distributions in the conduction and valence bands. At 77K the conduction band degeneracy is 7 meV, and added to $2k_BT$ (one for electrons and one for holes) yields 20 meV. At 300K the conduction band degeneracy is 33 meV, which added to $2k_BT$ yields $\sim$ 80 meV. At both temperatures the valence band is not degenerate. These estimates of the widths of the lifetime minimum agree reasonably well with Fig. 3(a,b).

Our results indicate that increasing temperature has a profound impact on final-state optimization for Auger suppression. Future work will consider the importance of Auger suppression at temperatures intermediate between 77K and 300K. It appears from Fig. 3(b) that at 300K the final-state optimization has just ceased to be of any importance, suggesting that for this structure it may still be important at temperatures just slightly lower. We conclude by pointing out that the beneficial effects of the band structure shown in Fig. 1(b) on the loss via valence intersubband absorption[9] remain present even though the final-state optimization is weak.

This research was supported in part by the United States Air Force, Air Force Materiel Command, Phillips Laboratory (PL), Kirtland AFB New Mexico 87117-5777 (contract F29601-97-C0041).

#2830 - $15.00 US
Received October 8, 1997; Revised February 12, 1998